ELSEVIER

International Journal of Mass Spectrometry and Ion Processes 167/168 (1997) 69–78

International Journal of Mass Spectrometry and Ion Processes

Cross-sections for the electron impact ionization of ND_x ($x = 1-3$)

V. Tarnovsky[a,*], H. Deutsch[b], K. Becker[a,1]

[a]*Physics Department, City College of C.U.N.Y., New York, NY 10031, USA*
[b]*Fachbereich Physik, Ernst-Moritz-Arndt-Universität, D-17487 Greifswald, Germany*

Abstract

Absolute cross-sections for the electron impact ionization and dissociative ionization of the ND_3 molecule and the ND_2 and ND free radicals were measured from threshold to 200 eV using the fast neutral beam technique. The deuterated rather than protonated targets were used in this work to facilitate a better separation of the various product ions from a given parent in our apparatus. A common feature of all three targets studied in this work is a dominant parent ionization cross-section with absolute values (at 70 eV) of 1.21×10^{-16} cm^2 (ND_3^+), 1.44×10^{-16} cm^2 (ND_2^+) and 1.45×10^{-16} cm^2 (ND^+). Dissociative ionization processes for all three targets are less significant, with a single dissociative process dominating in each case, the removal of a single D atom ($ND_x + e^- \rightarrow ND_{x-1}^+ + D + 2e^-$). The cross-section for this dominant dissociative ionization channel decreases from 1.03×10^{-16} cm^2 for ND_2^+/ND_3 to 0.85×10^{-16} cm^2 for ND^+/ND_2 to 0.40×10^{-16} cm^2 for N^+/ND. The measured appearance energies for the various fragment ions indicate that all fragment ions, except for D^+, are formed with little excess kinetic energy. Our experimental data for ND_3 are compared with existing experimental and theoretical data for NH_3.[2] Published by Elsevier Science B.V.

Keywords: Cross-sections; Electron impact ionization; ND_x ($x = 1-3$)

1. Introduction

Ammonia (NH_3) is a major constituent of the atmospheres of the planets Jupiter, Saturn, Uranus and Neptune. NH_3 is also employed as a propellant fuel in rocket and satellite thrusters using arc-heated discharges to generate high velocities. In these applications, collisional ionization of the parent molecule, as well as of the NH_2 and NH free radicals, is very important in order to understand and model the chemical reaction pathways. NH_2 and NH radicals are produced efficiently via collisional dissociation and photodissociation of the parent NH_3 molecule. There is a reasonably broad collisional database for NH_3. Photoionization and electron impact ionization processes of NH_3 have been studied previously [1–16]. As far as the ionization of NH_3 is concerned, there are some discrepancies in the available electron impact data in terms of the absolute cross-sections, cross-section shapes and appearance energies of the various fragment ions. To our knowledge, no collisional data are available for the NH_2 and NH free radicals.

This paper reports the absolute partial cross-sections for the electron impact ionization and dissociative ionization of the ND_3 molecule and the ND_2 and ND free radicals from threshold to 200 eV using the fast neutral beam technique. We

* Corresponding author.

[1] Present address: Department of Physics and Engineering Physics, Stevens Institute of Technology, Hoboken, NJ 07030, USA.

[2] PACS numbers: 34.80 Gs, molecular excitation, ionization and dissociation by electron impact; 52.20 Fs, electron collisions in plasmas.

0168-3659/97/$17.00 Published by Elsevier Science B.V.
PII S0168-1176(97)00033-5

used the deuterated rather than protonated target species, as performed in our previous studies of CD_x ($x = 1-4$) and SiD_x ($x = 1-3$), to facilitate a better separation of the various product ions from a given parent [17,18] (the absolute ionization cross-sections are largely insensitive to isotope effects [8,19,20]). Estimates of the total single ionization cross-sections for all three ND_x targets based on our measured partial cross-sections are also presented and compared with other available total ionization cross-sections. Lastly, we also determined the appearance energies for the various parent and fragment ions, which are compared with other available data and with thermochemically determined minimum energies.

2. Experimental details

A detailed description of the fast beam apparatus used in our laboratory and of the experimental procedure employed in the determination of the absolute partial ionization cross-sections has been given previously [21–24]. A d.c. discharge biased at typically 2–3 kV through ND_3 served as the primary ion source. The primary ions were mass selected in a Wien filter and a fraction was neutralized by near-resonant charge transfer in a charge transfer cell filled with Xe. Xe, with an ionization energy of 12.14 eV [25], was found to be an appropriate charge neutralization target for all three ND_x ($x = 1-3$) targets with ionization energies of 10.16 eV (ND_3), 11.14 eV (ND_2) and 13.49 eV (ND) [25–27]. Similar to previous studies [22,28–30], efficient charge transfer was not critically dependent on an exact match of the ionization energies of the charge transfer partners. The residual ions were removed from the target gas beam by electrostatic deflection and most species in Rydberg states were quenched in a region of high electric field. The neutral beam was subsequently crossed at right angles by a well-characterized electron beam (5–200 eV beam energy, 0.5 eV FWHM energy spread, 0.03–0.4 mA beam current). The product ions were focused in the entrance plane of an electrostatic hemispherical analyzer which separated the ions of different charge-to-mass ratios (i.e. parent ions from fragment ions). The ions leaving the analyzer were detected by a channel electron multiplier (CEM). The well-established Kr or Ar absolute ionization cross-section served as a convenient normalization standard to place the relative cross-section functions on an absolute scale [22–24]. This was performed by using the Kr or Ar benchmark cross-section to calibrate the pyroelectric crystal. The calibrated detector, in turn, was then used to determine the flux of the neutral target beam in absolute terms. This procedure avoids the frequent and prolonged exposure of the delicate pyroelectric crystal to fairly intense ion beams [23,24].

We established for each target that all fragment ions (except for D^+, see discussion below) with an excess kinetic energy of less than 2.5 eV per fragment ion are collected and detected with 100% efficiency using a combination of in situ experimental studies and ion trajectory modelling calculations [28]. Furthermore, careful threshold studies revealed little evidence of the presence of excited target species (vibrationally excited species, metastables and species in high-lying Rydberg states) in the incident neutral ND_x ($x = 1-3$) beams. In addition to these experimental checks, which are necessary for any target studied using the fast beam technique in order to ensure that the measured cross-sections are free from systematic uncertainties to the maximum extent possible [22–24], we also carried out all experimental checks pertaining specifically to hydrogen- and deuterium-containing targets as described in detail in Ref. [17].

We found little evidence of the presence of D^+ fragment ions from the dissociative ionization of all three ND_x targets. On the other hand, ion trajectory modelling calculations suggest significant losses of D^+ fragment ion from ND_x for excess kinetic energies as low as 0.5 eV per fragment ion, similar to that found previously for the SiD_x ($x = 1-3$) radicals [18]. Syage [16] determined

the kinetic energies for the various fragment ions produced by dissociative electron impact ionization of NH_3 and found an average kinetic energy of 1.4 eV for the H^+ fragment ions and a distribution which showed few fragment ions with kinetic energies below 0.5 eV. If we assume a similar kinetic energy distribution for the D^+ fragment ions from ND_3, it is obvious that it is difficult, if not impossible, to determine reliable absolute partial D^+ ionization cross-sections for any of the ND_x targets using our experimental approach. Therefore no quantitative data for D^+ formation from any of the ND_x target species ($x = 1-3$) are reported in this paper.

3. Results and discussion

For each of the three targets, we first measured the relative partial parent ionization cross-section from threshold to 200 eV, followed by a measurement of the relative partial cross-sections for the corresponding fragment ions. All measurements followed the previously described experimental procedure [22–24,28]. In all cases studied here, the measurements were limited to singly charged ions, since cross-sections for the formation of doubly charged ions were found to be at or below the detection sensitivity of our apparatus (peak cross-sections below 0.05×10^{-16} cm^2). The parent ionization cross-sections were then placed on an absolute scale by normalization to the well-known Kr or Ar benchmark cross-section as discussed above. All dissociative ionization cross-sections were subsequently normalized to the parent ionization cross-section for a given target. In all cases, careful threshold studies were carried out to check for the presence of excited species in the incident neutral beam and to determine the appearance energies for the various product ions. This is particularly crucial for dissociative ionization processes, since the appearance energy, when compared with thermochemical and spectroscopic data for the formation of a particular fragment ion, provides information about the (minimum) excess kinetic energy with which the fragment ion is formed.

The absolute cross-sections were determined with uncertainties of ± 15% for the parent ionization cross-sections and ± 18% for the dissociative ionization cross-sections. These error margins, which are similar to those quoted previously for the ionization cross-sections measured for other free radicals in the same apparatus [22–24,28], include statistical uncertainties and all known sources of systematic uncertainties.

3.1. Measured partial ionization cross-sections for ND_3

Fig. 1 shows the absolute cross-sections for the formation of ND_3^+ and ND_2^+ ions from ND_3 from threshold to 200 eV. The peak cross-section for the formation of ND^+ fragment ions from ND_3 was found to be slightly less than 0.1×10^{-16} cm^2 in good agreement with the results of Bederski et al. [7] and Syage [16] for the NH^+/NH_3 cross-section. By contrast, Märk et al. [8] report an NH^+/NH_3 cross-section which is only half this value, whereas the corresponding cross-section of Crowe and McConkey [9] is roughly three times larger than this value. Peak cross-sections for the other singly charged fragment ions (D^+, N^+) and cross-sections for multiply charged ions were found to be even smaller than 0.1×10^{-16} cm^2. Our measured partial ND_3^+ and ND_2^+ cross-sections at 70 eV are $(1.21 \pm 0.19) \times 10^{-16}$ cm^2 (ND_3^+) and $(1.03 \pm 0.19) \times 10^{-16}$ cm^2 (ND_2^+). The cross-section values are also listed in Table 1 for easier reference. It should be noted that the cross-sections in Table 1 represent the average of several individual data runs. The cross-section tables (with particular emphasis on the low energy regime) are presented primarily for the convenience of practitioners who use these cross-section data for modelling purposes or other applications. Also shown in Fig. 1 is the sum of the two partial ionization cross-sections (which represents a lower limit

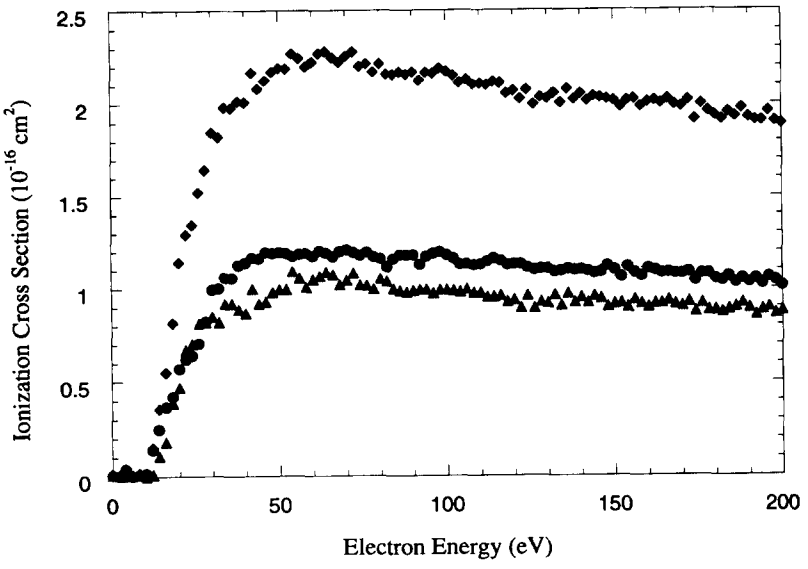

Fig. 1. Absolute cross-sections for the formation of the ND_3^+ parent ion (●) and the ND_2^+ fragment ion (▲) from ND_3 as a function of the electron energy. Also shown is the sum of the two measured partial ionization cross-sections (◆).

of the total ND_3 ionization cross-section, see discussion below). Our measured parent ND_3^+ ionization cross-section is in good agreement with most other recent measurements [7–9,16] in terms of the absolute cross-section value. On the other hand, there are some discrepancies concerning the cross-section shape. Our measured shape agrees well with the shapes reported by Bederski et al. [7], Märk et al. [8] and Crowe and McConkey [9], but we do not find any evidence of the double-peak structure reported by Syage [16]. Our measured cross-section shape for the ND_2^+ fragment ion is in good agreement with most of the other recently reported NH_2^+ results.

Based on our measured partial ND_3^+ and ND_2^+ ionization cross-sections and estimates and/or upper limits for the ND^+, N^+ and D^+ partial ionization cross-sections (see above), we find a total single ND_3 ionization cross-section of 2.4×10^{-16} cm^2 at 70 eV. Since the cross-sections for the formation of multiply charged parent and fragment ions from ND_3 are very small compared with the single ionization cross-sections [15,16], the total single ND_3 ionization cross-section is virtually identical to the total ND_3 ionization cross-section. Our value of 2.4×10^{-16} cm^2 is in excellent agreement with the NH_3 data of Bederski et al. [7] (2.3×10^{-16} cm^2), Märk et al. [8] (2.05×10^{-16} cm^2), Crowe and McConkey [9] (2.4×10^{-16} cm^2) and Syage [16] (2.35×10^{-16} cm^2). Our measured shape is also in good agreement with the shapes reported by these workers. We note that two other experimentally determined total NH_3 ionization cross-sections [14,15] are somewhat larger (3×10^{-16} cm^2 at 70 eV), although there is agreement between most reported total ionization cross-sections within their quoted combined uncertainties. It is interesting that the larger cross-section value is supported by the recent BEB calculation of Kim and coworkers [31] as well as by a more simplistic modified additivity rule [32]. In addition, there is a semi-empirical theory by Khare and Meath [33] which predicts a total NH_3 ionization cross-section of 2.7×10^{-16} cm^2 at 70 eV, roughly halfway between the two groups of experimentally determined cross-sections.

The measured appearance energy of the ND_3^+ parent ion of 10.3 ± 0.5 eV is very close to the known 10.16 eV ionization energy of ND_3 in its vibrational ground state [25–27]. The

Table 1
Measured partial ionization cross-sections for the formation of ND_3^+ and ND_2^+ from ND_3 as a function of the electron energy

Electron energy (eV)	Ionization cross-section (10^{-16} cm^2)	
	ND_3^+/ND_3	ND_2^+/ND_3
11.0	0.02	
12.0	0.04	
13.0	0.08	
14.0	0.13	
15.0	0.19	
16.0	0.27	0.04
17.0	0.35	0.16
18.0	0.43	0.28
19.0	0.50	0.39
20.0	0.58	0.50
22.0	0.69	0.59
24.0	0.78	0.66
26.0	0.86	0.72
28.0	0.93	0.77
30.0	1.00	0.82
35.0	1.07	0.87
40.0	1.14	0.92
45.0	1.18	0.97
50.0	1.20	1.00
60.0	1.22	1.02
70.0	1.21	1.03
80.0	1.20	1.01
90.0	1.19	1.00
100.0	1.17	0.98
120.0	1.14	0.95
140.0	1.11	0.92
160.0	1.10	0.90
180.0	1.07	0.89
200.0	1.03	0.87

near-threshold regions of the ND_3^+ and ND_2^+ cross-sections are shown in Fig. 2. We found no evidence of an extended curvature in the near-threshold region of the ND_3^+ cross-section or of a significant shift of the measured appearance energy to lower values. This indicates that the vibrational excitation of the ND_3 radicals in the target beam is negligible and there is no appreciable contamination of the target beam due to the presence of metastable ND_3 radicals or ND_3 radicals in long-lived Rydberg states. The measured appearance energy of the ND_2^+ fragment ions from ND_3 of 15.9 ± 0.7 eV is only marginally higher than the thermochemical minimum energy of 15.74 eV required for the formation of this fragment ion [25–27]. This indicates that the ND_2^+ fragment ions are formed with little excess kinetic energy. This is in accordance with the more quantitative finding of Syage [16] who determined an average kinetic energy of the NH_2^+ fragments from NH_3 of 0.026 eV using time-of-flight techniques. Syage [16] found slightly higher average kinetic energies for the NH^+ (0.22 eV), N^+ (0.31 eV) and H^+ (1.39 eV) fragment ions. If we assume similar values for the excess kinetic energies of the various deuterated fragment ions from ND_3, it is obvious that our apparatus is capable of detecting ND^+ and N^+ fragment ions with 100% efficiency, whereas we would lose a significant fraction of D^+ fragment ions. Our measured appearance energy for the ND_3^+ parent ion is in good agreement with all other previously reported appearance energies for this ion.

3.2. Measured partial ionization cross-sections for the ND_2 and ND free radicals

Fig. 3 shows the absolute cross-sections for the formation of ND_2^+ and ND^+ ions from the ND_2 free radical from threshold to 200 eV. The peak cross-sections for the formation of other singly charged fragment ions (D^+, N^+) and the cross-sections for multiply charged ions were found to be less than 0.1×10^{-16} cm^2. We find cross-sections of $(1.44 \pm 0.22) \times 10^{-16}$ cm^2 (ND_2^+) and $(0.85 \pm 0.15) \times 10^{-16}$ cm^2 (ND^+) at 70 eV. The cross-section shapes are very similar to the shapes of the ND_3 partial ionization cross-sections shown in Fig. 1. Also shown in Fig. 3 is the sum of the two partial ionization cross-sections (which represents a lower limit of the total ND_2 ionization cross-section, see discussion below and earlier for ND_3). Table 2 presents our measured ND_2 ionization cross-sections in tabulated form for convenient quantitative reference. The measured appearance energy of the ND_2^+ parent ions of 11.5 ± 0.5 eV is close to the known ND_2 ionization energy of 11.14 eV in its vibrational ground state. Threshold studies

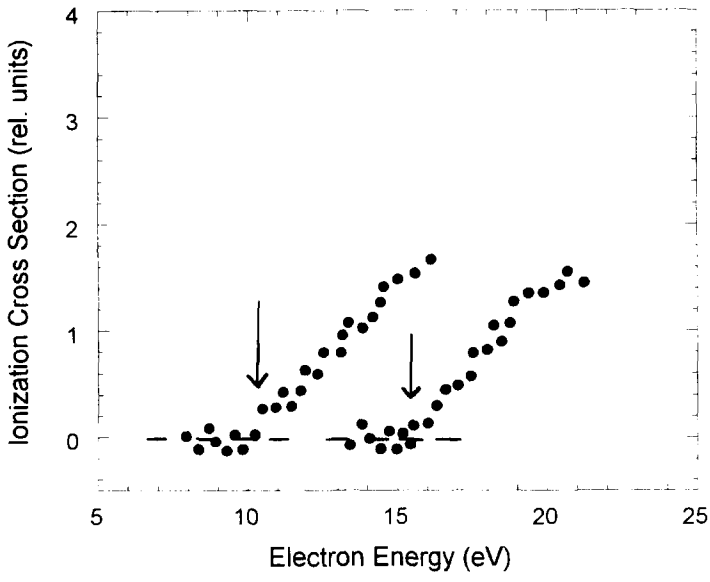

Fig. 2. Near-threshold region of the ND_3^+ and ND_2^+ partial ionization cross-section. The vertical arrows refer to the ionization energy of ND_3 (first arrow) and to the thermochemically calculated minimum energy for the formation of the ND_2^+ fragment ions from ND_3 (second arrow).

revealed little evidence of an extended curvature in the near-threshold region or of a shift of the measured appearance energy to a value significantly lower than the known ionization energy. This indicates that the vibrational excitation of the ND_2 radicals in the target beam is negligible and there is no appreciable contamination of the target beam due to the presence of metastable ND_2 radicals or ND_2 radicals in long-lived Rydberg states (similar to that observed in the case of ND_3). The measured appearance energy of the ND^+ fragment ions from ND_2 of 18.3 ± 0.7 eV is slightly higher than the

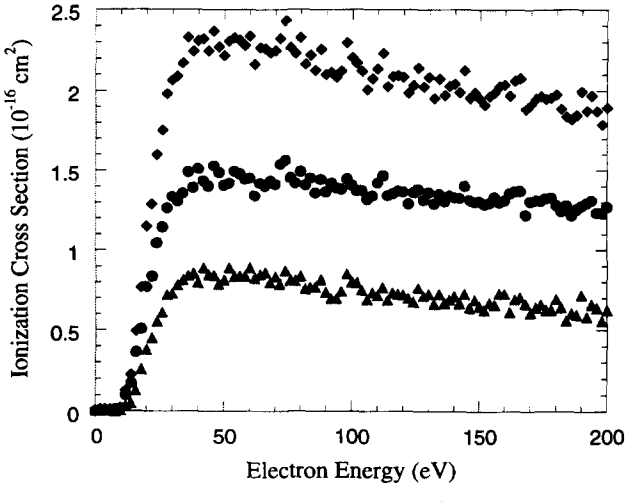

Fig. 3. Absolute cross-sections for the formation of the ND_2^+ parent ion (●) and the ND^+ fragment ion (▲) from ND_2 as a function of the electron energy. Also shown is the sum of the two measured partial ionization cross-sections (◆).

Table 2
Measured partial ionization cross-sections for the formation of ND_2^+ and ND^+ from ND_2 as a function of the electron energy

Electron energy (eV)	Ionization cross-section (10^{-16} cm^2)	
	ND_2^+/ND_2	ND^+/ND_2
11.0	< 0.01	
12.0	0.09	
13.0	0.17	
14.0	0.25	
15.0	0.32	
16.0	0.38	
17.0	0.45	
18.0	0.52	0.04
19.0	0.58	0.15
20.0	0.65	0.28
22.0	0.77	0.40
24.0	0.90	0.52
26.0	1.03	0.62
28.0	1.17	0.67
30.0	1.30	0.72
35.0	1.36	0.76
40.0	1.41	0.80
45.0	1.43	0.83
50.0	1.45	0.85
60.0	1.44	0.86
70.0	1.44	0.85
80.0	1.43	0.83
90.0	1.42	0.80
100.0	1.40	0.78
120.0	1.36	0.72
140.0	1.32	0.68
160.0	1.30	0.65
180.0	1.28	0.63
200.0	1.27	0.60

thermochemical minimum energy of 17.6 eV required for the formation of this fragment ion [25–27]. This indicates that the ND^+ fragment ions are formed with little excess kinetic energy.

Fig. 4 shows the absolute cross-sections for the formation of ND^+ and N^+ ions from the ND free radical from threshold to 200 eV. The peak cross-section for the formation of D^+ fragment ions was found to be less than 0.1×10^{-16} cm^2. Cross-sections for multiply charged ions were even smaller. We find cross-sections at 70 eV of $(1.45 \pm 0.23) \times 10^{-16}$ cm^2 (ND^+) and $(0.40 \pm 0.07) \times 10^{-16}$ cm^2 (N^+). Also shown in Fig. 4 is the sum of the two partial ionization cross-sections (which represents a lower limit of the total ND ionization cross-section, see discussion below and earlier for ND_3). The cross-section shapes are very similar to the shapes of the ND_3 and ND_2 partial ionization cross-sections shown in Figs. 1 and 3. Table 3 presents the measured ND partial ionization cross-sections averaged over several individual data runs in tabulated form for convenient quantitative reference. The measured appearance energy of the ND^+ parent ions of 13.6 ± 0.5 eV is close to the well-known ionization energy of 13.49 eV of ND in its vibrational ground state. We found little evidence of an extended curvature in the near-threshold region or of a significant shift of the measured appearance energy to lower values. This indicates that the vibrational excitation of the ND radicals in the target beam is negligible and there is no appreciable contamination of the target beam due to the presence of metastable ND radicals or ND radicals in long-lived Rydberg states (similar to that observed in the case of ND_3). The measured appearance energy of the N^+ fragment ions from ND of 18.3 ± 0.7 eV is slightly higher than the thermochemical minimum energy of 17.7 eV [25–27] required for the formation of this fragment ion. This indicates that the N^+ fragment ions are formed with little excess kinetic energy.

Based on the measured partial ionization cross-sections for ND_2 and ND, combined with estimates and/or upper limits for the unobserved fragment ions (N^+ and D^+ in the case of ND_2 and D^+ in the case of ND), we find total (single) ND_2 and ND ionization cross-section values at 70 eV of 2.4×10^{-16} cm^2 (ND_2) and 1.9×10^{-16} cm^2 (ND). These values are in very good agreement with the predictions of the modified additivity rule of Deutsch et al. [32] (2.4×10^{-16} cm^2 (NH_2) and 2.1×10^{-16} cm^2 (NH)).

4. Summary and conclusions

We used the fast beam technique to measure the partial ionization cross-sections for the ND_3

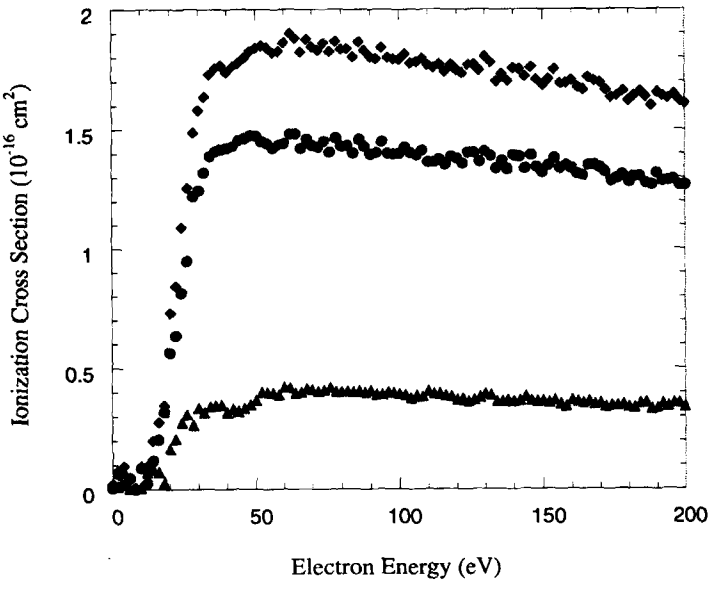

Fig. 4. Absolute cross-sections for the formation of the ND^+ parent ion (●) and the N^+ fragment ion (▲) from ND as a function of the electron energy. Also shown is the sum of the two measured partial ionization cross-sections (◆).

molecule and the ND_2 and ND free radicals from threshold to 200 eV. Four observations should be noted:

1. for all three targets, parent ionization is the dominant process and the most prominent dissociative ionization channel is that in which one D atom is removed, i.e. $ND_x \rightarrow ND^+_{x-1} + D$;
2. the cross-sections for the formation of the parent ions have similar values of about $(1.2–1.4) \times 10^{-16}$ cm^2 at 70 eV;
3. the cross-section for the formation of the dominant fragment ion decreases from 1.03×10^{-16} cm^2 for ND_2^+/ND_3 to 0.85×10^{-16} cm^2 for ND^+/ND_2 to 0.40×10^{-16} cm^2 for N^+/ND at 70 eV;
4. the measured appearance energies for the various fragment ions indicate that most fragment ions (except for D^+) are formed with little excess kinetic energy.

There are some notable similarities between the present ND_x data and the previously measured SiD_x and CD_x ($x = 1–3$) data [17,18]:

1. parent ionization is dominant in all cases and the parent ionization cross-section has essentially the same absolute value for all targets within a given AD_x family (where A ≡ Si, C or N);
2. one dissociative ionization channel, the removal of a single D atom, dominates in all cases;
3. all fragment ions (except for D^+) appear to be formed with little excess kinetic energy.

There is one notable difference between the data for CD_x and ND_x on the one hand and SiD_x on the other. In the case of SiD_x, the cross-section for the dominant dissociative ionization channel has the same value for all SiD_x targets, whereas we found a systematic decrease in the dominant dissociative ionization cross-section with decreasing value of x for CD_x and ND_x, i.e. the ND^+/ND_2 and CD^+/CD_2 cross-sections are smaller than the ND_2^+/ND_3 and CD_2^+/CD_3 cross-sections, whereas the N^+/ND and C^+/CD cross-sections are even smaller.

Lastly, the total (single) ionization cross-section for ND_3, derived from our measured

Table 3
Measured partial ionization cross-sections for the formation of ND^+ and N^+ from ND as a function of the electron energy

Electron energy (eV)	Ionization cross-section (10^{-16} cm^2)	
	ND^+/ND	N^+/ND
14.0	0.04	
15.0	0.12	
16.0	0.20	
17.0	0.28	
18.0	0.35	0.03
19.0	0.43	0.10
20.0	0.52	0.16
22.0	0.68	0.22
24.0	0.82	0.25
26.0	0.95	0.28
28.0	1.08	0.30
30.0	1.22	0.32
35.0	1.32	0.33
40.0	1.41	0.34
45.0	1.44	0.37
50.0	1.46	0.38
60.0	1.46	0.40
70.0	1.45	0.40
80.0	1.45	0.40
90.0	1.43	0.39
100.0	1.42	0.38
120.0	1.39	0.37
140.0	1.36	0.35
160.0	1.32	0.34
180.0	1.30	0.33
200.0	1.28	0.32

partial ionization cross-sections, is in good agreement with most of the measured NH_3 total ionization cross-sections available in the literature. However, two measurements reported slightly larger cross-sections which, in turn, are supported by two theoretical predictions. The experimentally determined ND_2 and ND total single ionization cross-sections are in excellent agreement with predictions from the modified additivity rule.

Acknowledgements

This work was supported by the National Aeronautics and Space Administration (NASA) through Grant No. NAGW-4118. One of us (V.T.) would also like to acknowledge partial support by the Division of Chemical Sciences, Office of Basic Energy Science, Office of Energy Research, US Department of Energy in the early stages of this work. The authors wish to thank Professor T.D. Märk, Dr R. Basner and Dr M. Schmidt for many helpful discussions.

References

[1] J.A.R. Samson, G.N. Haddad, L.D. Kilcoyne, J. Chem. Phys. 87 (1987) 6416.
[2] G.R. Wright, M.J. Van der Wiel, C.E. Brion, J. Phys. B 10 (1977) 1863.
[3] P.L. Kronebusch, J. Berkowitz, Int. J. Mass Spectrom. Ion Processes 22 (1976) 283. E. McCulloh, Int. J. Mass Spectrom. Ion Processes 21 (1976) 333.
[4] J.W. Rabalais, L. Karlsson, L.O. Werme, T. Berkmark, K. Siegbahn, J. Chem. Phys. 58 (1973) 3370.
[5] M.J. Weiss, G.M. Lawrence, J. Chem. Phys. 53 (1970) 214. G.R. Branton, D.C. Frost, F.G. Herring, C.A. McDowell, I.A. Stenhouse, Chem. Phys. Lett. 3 (1969) 581. A.W. Potts, W.C. Price, Proc. R. Soc. London Ser. A 326 (1972) 181.
[6] T.J. Xia, T.S. Chien, C.Y. Robert Wu, D.L. Judge, J. Quant. Spectrosc. Radiat. Transfer 45 (1991) 77. V.H. Diebeler, J.A. Walker, H.M. Rosenstock, J. Res. Natl. Bur. Stand A 70 (1966) 459. K. Watanabe, J.R. Mollt, J. Chem. Phys. 26 (1957) 1773. K. Watanabe, J. Chem. Phys. 22 (1954) 1564.
[7] K. Bederski, L. Wojcik, B. Adamczyk, Int. J. Mass Spectrom. Ion Processes 35 (1980) 171.
[8] T.D. Märk, F. Egger, M. Cheret, J. Chem. Phys. 67 (1977) 3795.
[9] A. Crowe, J.W. McConkey, Int. J. Mass Spectrom. Ion Processes 24 (1977) 181.
[10] J. Gomet, C.R. Acad. Sci. Ser. B 281 (1975) 627.
[11] L.E. Melton, J. Chem. Phys. 45 (1966) 4414.
[12] M.M. Mann, A. Hustruid, J.T. Tate, Phys. Rev. 58 (1940) 340.
[13] R. Locht, C. Servais, M. Ligot, F. Derwa, J. Momigny, Chem. Phys. 123 (1988) 443. R. Locht, C. Servais, M. Ligot, M. Davister, J. Momigny, Chem. Phys. 125 (1988) 425. R. Locht, J. Momigny, Chem. Phys. 127 (1988) 435.
[14] N. Djuric, D. Belic, M. Kurepa, J.U. Mack, J. Rothleitner, T.D. Märk, Contributed Papers, in: S. Datz (Ed.), XIIth International Conference on the Physics of Electronics and Atomic Collisions (ICPEAC), Gatlinburg, TN, USA, North Holland Publ. Comp., Amsterdam, 1981, p. 384.
[15] M.V.V.S. Rao, S.K. Srivastava, J. Phys. B 25 (1992) 2175.
[16] J.A. Syage, J. Chem. Phys. 97 (1992) 6085.
[17] V. Tarnovsky, A. Levin, H. Deutsch, K. Becker, J. Phys. B 29 (1996) 139.
[18] V. Tarnovsky, H. Deutsch, K. Becker, J. Chem. Phys. 105 (1996) 6815.
[19] T.D. Mark, F. Egger, J. Chem. Phys. 67 (1977) 2629.
[20] R. Basner, M. Schmidt, H. Deutsch, V. Tarnovsky, A. Levin, K. Becker, J. Chem. Phys. 103 (1995) 211.

[21] R.C. Wetzel, F.A. Biaocchi, T.R. Hayes, R.S. Freund, Phys. Rev. A 35 (1987) 559.
[22] R.S. Freund, R.C. Wetzel, R.J. Shul, T.R. Hayes, Phys. Rev. A 41 (1990) 3575.
[23] V. Tarnovsky, K. Becker, Z. Phys. D 22 (1992) 603.
[24] V. Tarnovsky, K. Becker, J. Chem. Phys. 98 (1993) 7868.
[25] S.G. Lias, J.E. Bartmess, J.F. Liebman, J.L. Holmes, R.D. Levine, W.G. Mallard, J. Phys. Chem. Ref. Data 17 (1988) 1.
[26] D.D. Wagman, W.H. Evans, V.B. Parker, R.H. Schumm, I. Halow, S.M. Bailey, K.L. Chuney, R.L. Nutall, J. Phys. Chem. Ref. Data 11 (1982) 1.
[27] M.W. Chase Jr., K.A. Davis, J.R. Downey, D.J. Frurip, R.A. McDonald, A.N. Syverud, J. Phys. Chem. Ref. Data 14 (1985) 1.
[28] V. Tarnovsky, P. Kurunczi, D. Rogozhnikov, K. Becker, Int. J. Mass Spectrom. Ion Processes 128 (1993) 181.
[29] V. Tarnovsky, A. Levin, K. Becker, J. Chem. Phys. 102 (1995) 770.
[30] V. Tarnovsky, A. Levin, K. Becker, J. Chem. Phys. 100 (1994) 5626.
[31] W. Hwang, Y.-K. Kim, M.E. Rudd, J. Chem. Phys. 104 (1996) 2956. Y.-K. Kim, M.E. Rudd, Phys. Rev. A 50 (1994) 3954.
[32] H. Deutsch, K. Becker, T.D. Mark, Int. J. Mass Spectrom. Ion Processes, in press.
[33] S.P. Khare, W.J. Meath, J. Phys. B 20 (1987) 2102, and references cited therein.